Inorg. Chem. **2002**, *41*, 1837–1844

Unique Reactivity of a Tetradentate N_2S_2 Complex of Nickel: Intermediates in the Production of Sulfur Oxygenates

Vincent E. Kaasjager,[†] Elisabeth Bouwman,*[,†] S. Gorter,[†] Jan Reedijk,[†] Craig A. Grapperhaus,[‡] Joseph H. Reibenspies,[‡] Jason J. Smee,[‡] Marcetta Y. Darensbourg,[‡] Agnes Derecskei-Kovacs,[§] and Lisa M. Thomson[§]

Gorlaeus Laboratories, Leiden Institute of Chemistry, P.O. Box 9502, 2300 RA Leiden, The Netherlands, Department of Chemistry, Texas A&M University, College Station, Texas 77843, and Laboratory for Molecular Simulation, Texas A&M University, College Station, Texas 77843

Received July 23, 2001

Complex **1** [(*N*,*N*′-dimethyl-*N*,*N*′-bis(2-sulfanylethyl)ethylenediamine)nickel(II)], previously shown to react with H_2O_2 to produce the fully oxygenated disulfonate **5** [diaqua(*N*,*N*′-dimethyl-*N*,*N*′-bis(2-sulfonatoethyl)ethylenediamine)-nickel(II)], has been explored in detail to explain the observed reactivity of this compound and to discern intermediates in the oxygenation reaction. Reaction of **1** with 1 equiv of methyl iodide results in the monomethylated square-planar nickel complex **2** {[(*N*,*N*′-dimethyl-*N*-(2-sulfanylethyl)-*N*′-(2-methylthioethyl)(ethylenediamine)nickel(II)] iodide}, while a slight excess of methyl iodide results in the dimethylated complex **3** [diiodo(*N*,*N*′-dimethyl-*N*,*N*′-bis(2-methylthioethyl)ethylenediamine)nickel(II)], an X-ray structure of which has shown that the nickel ion is in an octahedral $N_2S_2I_2$ environment. Crystal data of **3**: monoclinic, $a = 8.865(3)$ Å, $b = 14.419(4)$ Å, $c = 14.389(6)$ Å, $\beta = 100.19(3)^\circ$, $V = 1810.2(12)$ Å^3, space group $P2_1/n$, $Z = 4$. The equatorial positions are occupied by the two *cis*-amine N-atoms and the coordinated iodides, while the axial positions are occupied by the thioether sulfur atoms. In organic solvents, the dithiolate complex **1** reacts with molecular oxygen or H_2O_2 to produce the mixed sulfinato/thiolato complex **4** [(*N*,*N*′-dimethyl-*N*-(2-sulfanylethyl)-*N*′-(2-sulfinatoethyl)(ethylenediamine)nickel(II)], and the fully oxidized product **5**. X-ray analysis of complex **4** reveals a square-planar geometry in which the nickel ion is coordinated by two *cis*-amine nitrogens, one thiolate sulfur donor, and one sulfinato sulfur donor. Crystal data of **4**: orthorhombic, $a = 11.659(2)$ Å, $b = 13.119(3)$ Å, $c = 16.869(3)$ Å, $V = 2580.2(9)$ Å^3, space group *Pbca*, $Z = 8$. This complex is the only intermediate in the oxygenation reaction that could be isolated, and it is shown to be further reactive toward O_2 to yield the fully oxidized product **5**. For a better understanding of the reactivity observed for **4**, DFT calculations have been undertaken, which show a possible reaction path toward the fully oxidized product **5**.

Introduction

The air sensitivity of transition-metal thiolate complexes typically results in ligand-based oxidation of RS^- to $RS^\bullet$, with subsequent complex degradation.[1] Nevertheless, there is a growing number of examples of reactions of O_2 or other O-atom sources with metal thiolate complexes in which complex integrity is retained. Several metal complexes are known in which *S*-oxygenates are formed, such as in certain cobalt, palladium, and nickel complexes.[1−10] This process is of interest in view of the possible oxygenation of the active

* To whom correspondence should be addressed. E-mail: bouwman@chem.leidenuniv.nl.
[†] Leiden Institute of Chemistry.
[‡] Department of Chemistry, Texas A&M University.
[§] Laboratory for Molecular Simulation, Texas A&M University.

(1) Grapperhaus, C. A.; Darensbourg, M. Y. *Acc. Chem. Res.* **1998**, *31*, 451.
(2) Adzamli, I. K.; Deutsch, E. *Inorg. Chem.* **1980**, *19*, 1366.
(3) Connick, W. B.; Gray, H. B. *J. Am. Chem. Soc.* **1997**, *119*, 11620.
(4) Cornman, C. R.; Stauffer, T. C.; Boyle, P. D. *J. Am. Chem. Soc.* **1997**, *119*, 5986.
(5) Tuntulani, T.; Musie, G.; Reibenspies, J. H.; Darensbourg, M. Y. *Inorg. Chem.* **1995**, *34*, 6279.
(6) Cocker, T. M.; Bachman, R. E. *Chem. Commun.* **1999**, 875.
(7) Mirza, S. A.; Day, R. O.; Maroney, M. J. *Inorg. Chem.* **1996**, *35*, 1992−1995.
(8) Schrauzer, G. N.; Zhang, C.; Chadha, R. *Inorg. Chem.* **1990**, *29*, 4104.
(9) Yamanari, K.; Kawamoto, T.; Kushi, Y.; Komorita, T.; Fuyuhiro, A. *Bull. Chem. Soc. Jpn.* **1998**, *71*, 2635.
(10) Cocker, T. M.; Bachman, R. E. *Inorg. Chem* **2001**, *40*, 1550.

10.1021/ic010784x CCC: $22.00 © 2002 American Chemical Society
Published on Web 03/03/2002

sites of certain sulfur-rich metalloenzymes.[1,11,12] For example, the X-ray crystal structure of the nitrosylated Fe−nitrile hydratase revealed cysteine oxygenates, in both sulfenic (RSO) and sulfinic (RSO_2) forms, coordinated to the iron atom in the active site. A similar environment is suggested for the Co-containing nitrile hydratase.[13]

The dioxygen uptake in the Ni−*cis*-dithiolate complexes [(*N*,*N*′-bis(2-sulfanylethyl-1,5-diazacyclooctane)nickel(II)] [Ni(bme-daco)] and [(*N*,*N*′-bis(2-sulfanyl-2-methylpropyl)-1,5-diazacyclooctane)nickel(II)] [Ni(bme*-daco)] resulted in the isolation of *S*-oxygenates ranging from monosulfenates to the disulfinato species, all S-bound to nickel.[14,15] In contrast, in the case of the [Ni(dsdm)] complex (**1**) with the acyclic N_2S_2 ligand *N*,*N*′-dimethyl-*N*,*N*′-bis(2-sulfanylethyl)ethylenediamine, Henderson et al.[16] showed that the reaction with H_2O_2 yielded the disulfonato species diaqua(*N*,*N*′-dimethyl-*N*,*N*′-bis(2-sulfonatoethyl)ethylenediamine)nickel(II) [Ni(dsdm-O_6)(H_2O)$_2$] (**5**), in which the sulfonato groups are bound to nickel through oxygen. The increased O-atom uptake of the more flexible ligand resulted in a change from a low-spin to a high-spin nickel ion accompanied by a geometry change from square planar to octahedral.

The reactivity of [Ni(dsdm)] has been investigated in detail, and the reactivity toward methyl iodide, hydrogen peroxide, and molecular oxygen is reported, as well as the crystal structures of two new nickel complexes. Density functional theory (DFT) calculations are used to account for the observed reactivity.

Experimental Section

Materials. Reagent-grade solvents were dried using standard techniques and freshly distilled before use. Reactions were carried out under anaerobic conditions, using standard Schlenk or glovebox techniques under argon or dinitrogen gas.

Chromatography. All of the neutral nickel complexes were purified and separated from reaction mixtures by chromatography through a 20 cm × 1 cm column of silica gel (60−200 mesh, Aldrich grade 922 or EM Science grade 22), with ethanol and methanol as eluents. In almost all cases a red-brown material ascribed to the trinuclear complex $[Ni_3(dsdm)_2]^{2+}$ was produced upon interaction with the silica gel, and stayed on top of the column.[14,17] The complexes eluted from the column in the following order: **5**, **1**, **4** (see below). The yield was determined by weight differences following removal of solvent in preweighed vials or flasks.

Physical Measurements. UV−vis spectra were recorded in solution on a Hewlett-Packard HP8452A diode array spectrophotometer or on a Perkin-Elmer Lambda 900 spectrophotometer using the diffuse reflectance technique, with MgO as a reference. On the latter apparatus solution spectra were obtained with the solvent in the reference beam. Infrared spectra were recorded as KBr pellets using an IBM IR/32 Fourier transform single-beam spectrophotometer or a Perkin-Elmer FT-IR Paragon 1000 spectrophotometer.

Positive-ion fast-atom bombardment mass spectra (FAB-MS) were recorded in thioglycerol and nitrobenzyl alcohol matrixes using a VG-70S spectrometer with a xenon source having a particle energy of 10 keV. Data were collected by a VG11-250J data system. Electron spray ionization mass spectra (ESI-MS) were collected by constant infusion of the sample in methanol/water with 1% HAc, performed on a Finnigan MAT 900 equipped with an electrospray interface (ESI). Elemental analyses were carried out on a Perkin-Elmer series II CHNS/O analyzer 2400, or performed by Gailbraith Laboratories, Inc., Knoxville, TN.

Table 1. Crystallographic Parameters of **3** and **4**·H_2O

	3	**4**·H_2O
empirical formula	$C_{10}H_{24}I_2N_2NiS_2$	$C_8H_{18}N_2NiO_2S_2{\cdot}H_2O$
fw	548.95	315.09
space group	*P*21/*n*	*Pbca*
a (Å)	8.865(3)	11.659(2)
b (Å)	14.419(4)	13.119(3)
c (Å)	14.389(6)	16.869(3)
β (deg)	100.19(3)	90
V (Å^3)	1810.2(12)	2580.2(9)
Z	4	8
ρ(calcd) (g/cm^3)	2.014	1.622
temp (K)	295	293
radiation (λ, Å)	Mo Kα (0.71073)	Cu Kα (1.54178)
abs coeff (mm^{-1})	4.66	5.175
R1[a] (wR[b]/wR2[c])	0.0367 (0.0435)	0.0421 (0.1082)

[a] $R1 = \sum||F_o| - |F_c||/\sum|F_o|$. [b] $wR = [\sum w(|F_o| - |F_c|)^2/\sum w|F_o|^2]^{1/2}$. [c] $wR2 = [\sum w(F_o^2 - F_c^2)^2/\sum w(F_o^2)^2]^{1/2}$

X-ray Crystal Structure Analysis. X-ray analysis of **3** was performed on an Enraf-Nonius CAD-4 diffractometer with graphite-monochromatized Mo Kα radiation and using a $\omega-2\theta$ scan. Atomic scattering factors and anomalous dispersion constants were taken from the *International Tables for X-ray Crystallography*, Vol. C.[18] The intensities of the reflections were corrected for Lorentz and polarization effects. The positions of the heavy atoms were determined from Patterson maps (DIRDIF[19]). The remainder of the non-hydrogen atoms were found in subsequent ΔF syntheses (XTAL[20]). Hydrogen atoms were placed at calculated positions. Full-matrix least-squares refinement on *F* of the positional and the anisotropic thermal parameters of the non-hydrogen atoms and of the positional parameters of the hydrogens, which were assigned fixed isotropic thermal parameters (XTAL),[20] was performed. A summary of crystal data and refinement results is given in Table 1. Geometric calculations and molecular graphics were performed with the PLATON package.[21]

X-ray crystallographic data of **4** were obtained on a Rigaku AFC5 single-crystal X-ray diffractometer operating at 50 kV and 180 mA, with Cu Kα radiation, equipped with a MSC LT cryostat. The

(11) Fontecilla-Camps, J. C. *Struct. Bonding* **1998**, *91*, 2.
(12) Maroney, M. J.; Davidson, G.; Allan, C. B.; Figlar, J. *Struct. Bonding* **1998**, *92*, 2.
(13) Nagashima, S.; Nakasako, M.; Dohmae, N.; Tsujimura, M.; Takio, K.; Okada, M.; Yohda, M.; Kamiya, N.; Endo, I. *Nat. Struct. Biol.* **1998**, *5*, 347.
(14) Buonomo, R. M.; Font, I.; Maguire, M. J.; Reibenspies, J. H.; Tuntulani, T.; Darensbourg, M. Y. *J. Am. Chem. Soc.* **1995**, *117*, 963.
(15) Farmer, P. J.; Solouki, T.; Mills, D. K.; Soma, T.; Russel, D. H.; Reibenspies, R. H.; Darensbourg, M. Y. *J. Am. Chem. Soc.* **1992**, *114*, 4601.
(16) Henderson, R. K.; Bouwman, E.; Spek, A. L.; Reedijk, J. *Inorg. Chem.* **1997**, *36*, 4616.
(17) Turner, M. A.; Driessen, W. L.; Reedijk, J. *Inorg. Chem.* **1990**, *29*, 3331.
(18) Wilson, A. J. C., Ed. *International tables for X-ray Crystallography*; Kluwer Academic Publishers: Dordrecht, The Netherlands, 1992; Vol. C.
(19) Beurskens, P. T.; Admiraal, G.; Beurskens, G.; Bosman, W. P.; Garcia-Granda, S.; Gould, R. O.; Smits, J. M. M.; Smykalla, C. *The DIRDIF program system*; Technical Report of the Crystallography Laboratory; University of Nijmegen: Nijmegen, The Netherlands, 1996.
(20) Hall, S. R.; King, G. S. D.; Stewart, J. M. *XTAL 3.4 User's Manual*; Universities of Western Australia and Maryland: Crawley, Western Australia, and College Park, MD, 1995.
(21) Spek, A. L. *PLATON. A multipurpose crystallographic tool*; Utrecht University: Utrecht, The Netherlands, 2000.

diffractometer control software, CTR, was supplied by Molecular Structure Corp. All crystallographic calculations were performed with the use of the SHELX-97 program against F^2.[22] X-ray experimental data for the complex are collected in Table 1.

Computational Details. Six nickel complexes were used in the computations: [Ni(dsdm)] (**1**), [Ni(dsdm-O_2)] (**4**), [Ni(dspm)] (dspm = *N*,*N*′-dimethyl-*N*,*N*′-bis(2-sulfanylethyl)propylenediamine), [Ni(dspm-O_2)] (dspm-O_2 = *N*,*N*′-dimethyl-*N*-(2-sulfanylethyl)-*N*′-(2-sulfinatoethyl)(propylenediamine)), and the pair [Ni(bme-daco)] and [Ni(mese-daco)] (mese-daco = 1-(sulfinatoethyl)-5-(sulfanylethyl)-1,5-diazacyclooctane). All compounds were fully optimized using DFT,[23] with the Becke3 hybrid exchange functional and the Lee−Yang−Parr correlational functional (B3LYP).[24] All calculations were performed with the Gaussian 98(G98)[25] suite of programs using a full double-ζ basis set[26] (D95) for C, N, and H atoms and a full double-ζ basis set plus one polarization function (D95*) on the O atoms. For the sulfur atoms, the Hay and Wadt effective core potential (ECP) (1s2s2p) with a double-ζ basis set[27−29] (LANL2DZ) plus a polarization function[30,31] (exponent 0.305) was used to properly describe the hypervalent character of the sulfur in the R_2SO_2 unit. For the Ni atom, a small core Hay and Wadt ECP5 (1s2s2p) was used with a double-ζ basis set that includes a description for the outer 4p function developed by Couty and Hall,[32] with a splitting of (341/3311/41). Coordinates for the starting geometries were taken from the crystal structure data, when available. The structure and energy for both the eclipsed and staggered conformations of the side arms (N−C−C−S) for all compounds were compared. Frequency calculations performed on all optimized structures confirmed that they are minima, i.e., that there are no imaginary frequencies. All energetics reported from theoretical results are enthalpy differences between two molecules or structures.

Syntheses. The syntheses of H_2dsdm,[33] [Ni(dsdm)] (**1**)[17] and [Ni(dsdm-O_6)(H_2O)$_2$] (**5**)[16] have been described in detail elsewhere.

[(*N*,*N*′-Dimethyl-*N*-(2-sulfanylethyl)-*N*′-(2-methylthioethyl)-(ethylenediamine)nickel(II)] Iodide, [Ni(Medsdm)]I (2). A solution of MeI (46 μL, 0.75 mmol, 1 equiv) in 20 mL of EtOH was added over the course of 1 h to a solution of 200 mg (0.75 mmol) of **1** in 30 mL of EtOH. The reaction mixture was stirred overnight, during which time no apparent color change took place. The solution was then reduced in volume to 10 mL, and ether was diffused into the solution, resulting in the precipitation of a dark brown solid. The solvent was decanted, and the solid was washed with diethyl ether (3 × 10 mL), resulting in 70% of a dark brown product. UV−vis (in methanol): λ_{max} (ϵ, cm^{-1} M^{-1}) 222 (21500), 259 (8054), 304 (6966), 472 (261), 608 (sh) nm. Anal. Calcd (Found) for $C_9H_{21}IN_2NiS_2$: C, 26.56 (26.60); H, 5.20 (5.28); N, 6.88 (6.59).

[Diiodo(*N*,*N*′-dimethyl-*N*,*N*′-bis(2-methylthioethyl)ethylenediamine)nickel(II)], [Ni(Me$_2$dsdm)I$_2$] (3). To a solution of 100 mg (0.38 mmol) of **1** in 30 mL of CH_3CN was added 3 equiv of MeI (75 μL, 1.13 mmol), with stirring. Allowing the reaction mixture to stand overnight resulted in a green-colored solution, which was reduced in volume to 5 mL. Diethyl ether was added, and the solution was stored at −20 °C, resulting in a green precipitate which was collected by filtration and washed with diethyl ether (3 × 5 mL), yielding 82% of a light-green product. Crystals suitable for X-ray analysis were grown in an acetonitrile/diethyl ether solution at room temperature. UV−vis (in methanol): λ_{max} (ϵ, cm^{-1} M^{-1}) 221 (35300), 266 (4100), 646 (19), 1084 (22) nm. Anal. Calcd (Found) for $C_{10}H_{24}I_2N_2NiS_2$: C, 21.88 (22.15); H, 4.41 (4.35); N, 5.10 (5.33).

Reaction of 1 with H_2O_2. In a typical experiment, 50 mg (0.19 mmol) of **1** was dissolved in 50 mL of ethanol at −76 °C. Solutions containing 2, 3, or 4 equiv of H_2O_2 (30% w/v aqueous) in 25 mL of ethanol were added dropwise to the cold solution of **1** over the course of 1 h. The resulting (yellow to green) solutions were brought to room temperature and concentrated by rotary evaporation. The remaining solid was chromatographed as described above. Product yields were determined for **4** and **5** only: 2 equiv of H_2O_2 (to 1 equiv of **1**), 10% **4**, 20% **5**; 3 equiv of H_2O_2, 16% **4**, 36% **5**; 4 equiv of H_2O_2, 8% **4**, 52% **5**.

Reaction of 1 with O_2. In a typical experiment, 36 mg (0.14 mmol) of **1** was dissolved in 80 mL of the appropriate solvent (methanol, acetonitrile, or dimethylformamide (DMF)) and stirred under 1 bar of O_2 for a given time. The solvent was removed by rotary evaporation, the remaining yellow solid was taken up in a minimum of methanol, and the products were separated by chromatography on a silica gel column. Reaction times and yields are shown in Table 5.

[(*N*,*N*′-Dimethyl-*N*-(2-sulfanylethyl)-*N*′-(2-sulfinatoethyl)(ethylenediamine)nickel(II) Monohydrate], [Ni(dsdm-O_2)]·H_2O (4·H_2O). This compound was eluted with methanol as the third fraction from the column as described above. Orange crystals suitable for X-ray crystal structure analysis were obtained by slow diffusion of ether into a concentrated ethanolic solution of **4**. FTIR peaks assigned to ν(SO): 1174(s) and 1039(s) cm^{-1}. UV−vis (in methanol): λ_{max} (ϵ, cm^{-1} M^{-1}) 224 (3917), 256 (2692), 298 (2856), 448 (268) nm. Anal. Calcd (Found) for $C_8H_{18}N_2NiO_2S_2$·H_2O: C, 30.50 (30.84); H, 6.40 (6.08); N, 8.89 (9.02).

Reaction of 4 with O_2. A solution of 38 mg (0.13 mmol) of **4** in dimethylformamide was stirred for 144 h under a pressure of 1 bar of dioxygen. After removal of the solvent the product was dissolved in methanol and purified by chromatography on a silica gel column, to yield 59% **5**.

Results and Discussion

Syntheses. The monomethylated compound **2** and the dimethylated compound **3** are easily obtained by reaction of **1** with methyl iodide (Scheme 1). For the synthesis of **2**, 1

(22) Sheldrick, G. *SHELXL-97. Program for Crystal Structure refinement*; University of Göttingen: Göttingen, Germany, 1997.
(23) Parr, R. G.; Yang, W. *Density-functional Theory of Atoms and Molecules*; Oxford University Press: Oxford, 1989.
(24) Becke, A. *J. Chem. Phys.* **1993**, *98*, 5648.
(25) Frisch, M. J.; Trucks, G. W.; Schlegel, H. B.; Scuseria, G. E.; Robb, M. A.; Cheeseman, J. R.; Zakrzewski, V. G.; Montgomery, J. A.; Stratmann, R. E.; Burant, J. C.; Dapprich, S.; Millam, J. M.; Daniels, A. D.; Kudin, K. M.; Strain, M. C.; Farkas, O.; Tomasi, J.; Barone, V.; Cossi, M.; Cammi, R.; Mennucci, B.; Pomelli, C.; Adamo, C.; Clifford, S.; Ochterski, J.; Petersson, G. A.; Ayala, P. Y.; Cui, Q. M., K.; Malick, D. K.; Rabuck, A. D.; Raghavachari, K.; Foresman, J. B.; Cioslowski, J.; Ortiz, J. V.; Stefanov, B. B.; Liu, G.; Liashenko, A.; Piskorz, P.; Komaromi, I.; Gomperts, R.; Martin, R. L.; Fox, D. J.; Keith, T.; Al-Laham, M. A.; Peng, C. Y.; Nanayakkara, A.; Gonzalez, C.; Challacombe, M.; Gill, P. M. W.; Johnson, B. G.; Chen, W.; Wong, M. W.; Andres, J. L.; Head-Gordon, M.; Replogle, E. S.; Pople, J. A. *Gaussian 98*; Gaussian, Inc.: Pittsburgh, 1998.
(26) Dunning, T.; Hay, P. In *Modern Theoretical Chemistry*; Schaefer, H. F., III, Ed.; Plenum: New York, 1976.
(27) Hay, P. J.; Wadt, W. R. *J. Chem. Phys.* **1985**, *82*, 270.
(28) Hay, P. J.; Wadt, W. R. *J. Chem. Phys.* **1985**, *82*, 284.
(29) Hay, P. J.; Wadt, W. R. *J. Chem. Phys.* **1985**, *82*, 299.
(30) Hollwarth, A.; Bohme, M.; Dapprich, S.; Ehlers, A. W.; Gobbi, A.; Jonas, V.; Kohler, K. F.; Stegmann, R.; Veldkamp, A.; Frenking, G. *Chem. Phys. Lett.* **1993**, *208*, 237.
(31) Hollwarth, A.; Bohme, M.; Dapprich, S.; Ehlers, A. W.; Gobbi, A.; Jonas, V.; Kohler, K. F.; Stegmann, R.; Veldkamp, A.; Frenking, G. *Chem. Phys. Lett.* **1994**, *224*, 603.
(32) Couty, M.; Hall, M. *J. Comput. Chem.* **1996**, *17*, 1359.
(33) Avdeef, A.; Hartenstein, F.; Chemotti, A. R.; Brown, J. A. *Inorg. Chem.* **1992**, *31*, 3701.

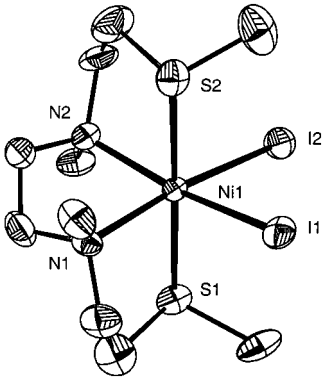

Figure 1. Thermal ellipsoid projection (at 30% probability) and atomic labeling of [Ni(Me_2dsdm)I_2].

Scheme 1

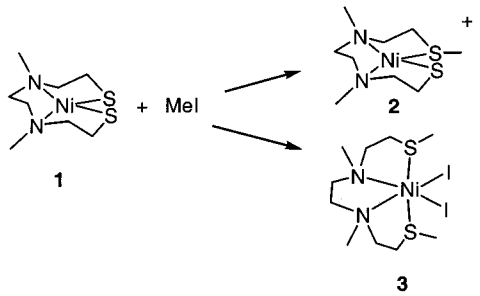

Scheme 2

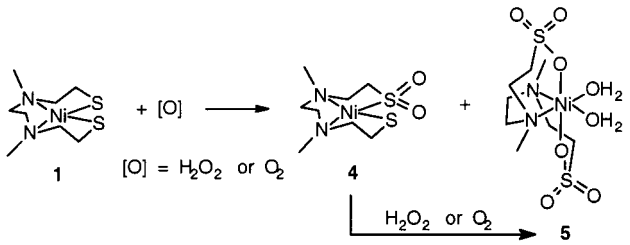

equiv of methyl iodide was used. During the overnight reaction no obvious color change was observed; however, in the synthesis of **3**, in which an excess of methyl iodide was used, a color change from brown to green occurred.

The reaction of [Ni(dsdm)] with H_2O_2 resulted in the isolation of two products, the monosulfinate **4** and the disulfonate **5**. The monosulfinate complex **4** could be isolated by using less than stoichiometric amounts of H_2O_2 and low temperatures. The same two products were obtained by reaction of **1** with dioxygen, a result not yet reported before, in a ratio depending on the solvent and reaction time. The obtained products were separated by column chromatography and are visualized in Scheme 2. The three new complexes have been characterized by elemental analysis and spectroscopic techniques. In addition, the structures of compounds **3** and **4** have been elucidated by X-ray analysis.

Description of the Structures. The molecular structure of **3** is depicted in Figure 1, and selected bond distances and angles are given in Table 2. The compound crystallizes in the space group $P2_1/n$, and the asymmetric unit contains a nickel ion in a distorted octahedral geometry. The nickel is coordinated by two *cis*-amine nitrogen donors and two axially coordinated *trans*-thioether donors, while two *cis*-

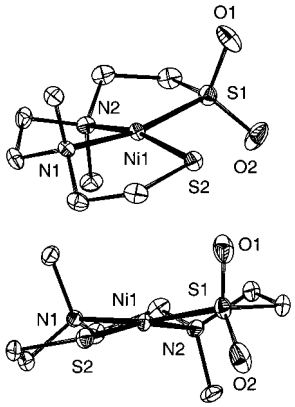

Figure 2. Two views of the thermal ellipsoid projection (at 30% probability) and atomic labeling of [Ni(dsdm-O_2)].

Table 2. Selected Bond Distances (Å) and Angles (deg) for **3**

Ni(1)−S(1)	2.427(2)	Ni(1)−N(2)	2.186(5)
Ni(1)−S(2)	2.425(2)	Ni(1)−I(1)	2.817(1)
Ni(1)−N(1)	2.167(4)	Ni(1)−I(2)	2.840(1)
S(1)−Ni(1)−N(1)	82.2(1)	I(1)−Ni(1)−S(2)	84.52(5)
S(1)−Ni(1)−N(2)	97.1(1)	I(1)−Ni(1)−N(1)	93.2(1)
S(2)−Ni(1)−N(1)	97.1(1)	I(1)−Ni(1)−N(2)	165.0(1)
S(2)−Ni(1)−N(2)	81.7(1)	I(2)−Ni(1)−S(1)	84.15(4)
S(1)−Ni(1)−S(2)	178.65(6)	I(2)−Ni(1)−S(2)	96.42(5)
N(1)−Ni(1)−N(2)	82.9(2)	I(2)−Ni(1)−N(2)	93.3(1)
I(1)−Ni(1)−I(2)	93.95(3)	I(2)−Ni(1)−N(1)	165.3(1)
I(1)−Ni(1)−S(1)	96.68(5)		

iodide ions complete the coordination sphere. The Ni−N bond distances of 2.186(5) and 2.167(4) Å are comparable to those found in the similar complex [Ni("$N_2Me_2S_2Me_2$")I_2] ("$N_2Me_2S_2Me_2$" = *N*,*N*′-dimethyl-*N*,*N*′-bis(2-methylthiophenyl)ethylenediamine) (2.171(9) Å), which contains two aromatic thioether donor ligands.[34] The observed identical nickel thioether bond distances of 2.425 Å in **3** are slightly longer than the 2.387 Å observed for [Ni("$N_2Me_2S_2Me_2$")-I_2]. The difference in these bond lengths can be ascribed to the more flexible aliphatic arm of **3** or could be due to the electronic difference of the aromatic thioether versus the aliphatic thioether. The *N*-methyl groups of **3, 4**, (vide supra) and **5**[16] are *transoidal* to one other, i.e., on different sides of the N−C−C−N best plane. In contrast, the [Ni(dsdm)] unit found in the trinuclear compound $[Ni_3(dsdm)_2]Cl_2 \cdot 2H_2O$, as well as the mononuclear compound [Ni(dspm)], contains a *cisoidal* configuration of the *N*-methyl groups.[17,35] An obvious difference is observed when the structure of **3** is compared with the analogous [Ni(Me_2bme-daco)]I_2 ([(*N*,*N*′-bis(3-thiabutyl)-1,5-diazacyclooctane)nickel(II)] diiodide) in which the N_2S_2 ligand remains in the equatorial coordination plane, due to the specific properties of the backbone.[36] In the latter complex the nickel ion remains in the low-spin state and the iodides are not coordinated.

The molecular structure of **4** is shown in Figure 2, and selected bond lengths and angles are listed in Table 3. The square-planar nickel ion is coordinated by two *cis*-amine

(34) Sellmann, D.; Prechtel, W.; Knoch, F.; Moll, M. *Z. Naturforsch.* **1992**, *47b*, 1411.
(35) Colpas, G. J.; Kumar, M.; Day, R. O.; Maroney, M. J. *Inorg. Chem.* **1990**, *29*, 4779.
(36) Mills, D. K.; Reibenspies, J. H.; Darensbourg, M. Y. *Inorg. Chem.* **1990**, *29*, 4364.

Table 3. Selected Bond Distances (Å) and Angles (deg) for **4**

Ni(1)−S(1)	2.119(1)	Ni(1)−N(2)	1.933(3)
Ni(1)−S(2)	2.149(1)	S(1)−O(1)	1.461(4)
Ni(1)−N(1)	1.940(3)	S(1)−O(2)	1.474(4)
S(1)−Ni(1)−S(2)	94.90(5)	N(2)−Ni(1)−S(2)	166.23(11)
N(1)−Ni(1)−S(2)	90.66(11)	O(1)−S(1)−Ni(1)	112.38(15)
N(2)−Ni(1)−S(1)	88.85(10)	O(2)−S(1)−Ni(1)	116.23(15)
N(2)−Ni(1)−N(1)	88.11(14)	O(1)−S(1)−O(2)	113.8(2)
N(1)−Ni(1)−S(1)	168.45(11)		

nitrogens, one thiolate sulfur donor, and one sulfinato sulfur donor. A significant distortion from square-planar geometry toward tetrahedral is observed; the tetrahedral twist of 17.5° is similar to that observed in [Ni(mese-daco)] (18.4°).[15]

The Ni(1)−S(1) distance of 2.119(1) Å from the oxygenated sulfur of complex **4** and the Ni(1)−S(4) distance of the thiolate ligand, 2.149(1) Å, are nearly the same. This outcome is ascribed to the following compensatory effects: (1) the decreased σ-donor ability of the sulfinato sulfur which weakens the $Ni-S_{sulfinate}$ bond should increase the bond distance, (2) the decreased radius of the oxidized sulfur (S^{2+}) compared to the thiolate sulfur (S^{2-}) should result in a decrease of the $Ni-S_{sulfinate}$ bond distance, and (3) the loss of the nickel−thiolate Ni(d_π)/S(p_π) antibonding interaction upon oxygenation would also serve to shorten the Ni−S bond.[37] The fact that the bond length decreases shows that the latter two effects dominate over the first one. Similar results have been observed for other nickel complexes containing both a sulfinate and a thiolate ligand.[1] The S−O distances of 1.46 Å in **4** are comparable to those in the disulfonate complex **5** (1.44−1.45 Å).[16]

An obvious difference between **4** and the related propylene-bridged complex [Ni(dspm-O_2)] is the orientation of the methyl groups on the amine nitrogens. The *N*-methyl groups are transoidal in **4**, while for [Ni(dspm-O_2)] a cisoidal conformation is observed.[38] The complex cocrystallizes with one water molecule hydrogen-bonded to a sulfinato oxygen of one molecule of **4**, with a distance of 2.776 Å. A channel of water molecules propagating parallel to the *ab* plane separates individual rows of the nickel complex as visualized in Figure S1 in the Supporting Information.

Spectroscopic Properties. The UV−vis data for the new complexes **2**−**4** in methanol are collected in Table 4, as well as those of the previously reported compounds **1** and **5**. For the monomethylated complex **2** a low-intensity transition is observed at 472 nm, with a shoulder at 608 nm. These can be tentatively assigned to d → d transitions from a low-spin five-coordinated nickel complex. On the basis of these spectroscopic data together with elemental analysis and mass spectroscopy, it can be assumed that **2**, in solution, is most likely a square-planar cationic nickel complex with a weakly coordinating iodide ion. The spectrum of the monosulfinate complex **4** is typical for a square-planar nickel complex with a d → d transition at 448 nm. The other observed absorptions in **2** and **4** can be assigned as ligand-to-metal charge-transfer (LMCT) transitions.[39] The nickel ions in the dimethylated compound **3** and the disulfonate complex **5** are in octahedral coordination as can be judged by the low-intensity transitions in the spectra at 1084 and 646 nm for **3** and at 1120, 653, and 386 nm for **5**.[40] The transition expected around 300 nm for **3** is obscured by high-intensity LMCT bands**.**

In the IR spectrum two strong bands are observed in the solid state for **4** at 1174 and 1039 cm^{-1}, comparable to those observed for [Ni(mese-daco)], and are assigned to ν(SO).[14]

Oxygenation Studies. As previously reported, 6 equiv of H_2O_2 reacts with **1** in ethanol to yield the disulfonate compound **5** exclusively.[16] Substoichiometric amounts of H_2O_2 in the range from 2 to 4 molar ratio with respect to nickel result in a mixture of products (Scheme 2), composed of the monosulfinate compound **4**, the disulfonate complex **5**, and also unreacted **1**. These complexes were separated by column chromatography. Using up to 6 equiv of H_2O_2 led to increased yields of **5**, while for the isolation of **4** an optimum yield was reached at 3 equiv of H_2O_2. No other intermediates could be isolated, even though the reactions were carried out at −76 °C and with high dilution.

While it was reported that no oxidized product was observed when solutions of [Ni(dsdm)] were exposed to air,[16] it appears that prolonged exposure of 1.7 mM solutions of this compound to pure dioxygen (1 bar and 22 °C) resulted in the formation of products identical to those described above, namely, **4**, **5**, and unreacted **1**. The results have been summarized in Table 5. Although several nickel sulfonate complexes are known,[6,41−43] this conversion from a thiolate to a sulfonate by reaction with molecular oxygen is unprecedented. Reactions carried out with singlet oxygen ($^1\Sigma O_2$) showed enhanced reactivity, but led to the same products with no other oxygenated species observed.

The product distribution of the monosulfinate complex **4** and the disulfonate compound **5** is solvent dependent. As can be seen in entries 1−3 of Table 5, acetonitrile is the optimal solvent for production of **4**; the use of dimethylformamide or MeOH results in smaller amounts of **4** due to different reaction rates. The highest degree of oxidation (and thus formation of **5**) is obtained in DMF, entry 1, whereas the lowest degree of oxidation is observed in methanol, entry 3. Similar results were observed by Mirza et al.,[44] who reported that the reaction of a nickel *trans*-dithiolate compound with molecular oxygen led to the oxidation of only one of the thiolates to a monosulfinate. As shown in Table 5, entry 4, the monosulfinate complex **4** shows further reactivity toward dioxygen, resulting in the disulfonate product **5**. Following the reaction in time with UV−vis spectroscopy in DMF as solvent, a decrease of concentration is observed for **4** as judged by the absorption at 455 nm. Simultaneously, an increase at 650 and 1100 nm attributable

(37) Farmer, P. J.; Reibenspies, J. H.; Lindahl, P. A.; Darensbourg, M. Y. *J. Am. Chem. Soc.* **1993**, *115*, 4665.
(38) Maroney, M. J. Private communication, 2001.
(39) Maroney, M. J.; Choudhurry, S. B.; Bryngelson, P. A.; Mirza, A. M.; Sherrod, M. J. *Inorg. Chem.* **1996**, *35*, 1073.
(40) Lever, A. B. P. *Inorganic Electronic Spectroscopy*, 2nd ed.; Elsevier: Amsterdam, 1984.
(41) Wieghardt, K.; Bossek, U.; Guttmann, M.; Weiss, J. *Z. Naturforsch., B* **1983**, *38*, 81.
(42) Smieja, J.; Place, H.; Brewer, K. J. *Acta Crystallogr.* **1991**, *C47*, 2455.
(43) Endres, H. Z. *Z. Anorg. Allg. Chem.* **1984**, *513*, 78.
(44) Mirza, S. A.; Pressler, M. A.; Kumar, M.; Day, R. O.; Maroney, M. J. *Inorg. Chem.* **1993**, *32*, 977.

Table 4. Spectroscopic and Physical Data of Compounds **1**−**5**

	1	**2**	**3**	**4**	**5**
IR[a] (ν(SO))				1039, 1174	1157, 1178, 1208, 1233
parent ion (m/z)	265[b]	279[c]	421[c]	297[b]	361[b]
d → d (nm) (ϵ)[d]	481 (250)	472 (260)	646 (19)	448 (270)	385 (11)
	345 (sh)	608 (sh)	1084 (22)		653 (7)
					1120 (8)

[a] KBr pellets. [b] FAB-MS. [c] ESI-MS. [d] ϵ in M^{-1} cm^{-1} with methanol as solvent.

Table 5. Product Distribution (%) for Reaction of **1** and **4** with O_2 in Different Solvents at 22 °C

entry	compound	solvent	**4** (%)	**5** (%)
1[a]	**1**	DMF	20	56
2[a]	**1**	CH_3CN	54	22
3[a]	**1**	CH_3OH	14	10
4[b]	**4**	DMF		59

[a] After 192 h of stirring of a 1.7 mM solution of **1**. [b] After 144 h of stirring of a 6.4 mM solution of **4**.

to the octahedral species **5** is observed. During this reaction no isosbestic points are formed, implying the formation of an intermediate species that quickly reacts further to the final disulfonato product **5**. In contrast, the monosulfinate complex [Ni(mese-daco)] does not react further with $^{3}\pi O_2$. However, with excited-state $^{1}\Sigma O_2$, [Ni(mese-daco)] reacts to form the disulfinato complex.[45] Reactions with molecular oxygen have also been described for [Ni(dspm)], which was shown to yield exclusively the monosulfinato compound [Ni(dspm-O_2)].[39] No further reactivity was observed, and this was explained on the basis of MO calculations. The result shown here for [Ni(dsdm)] is thus unique and does suggest the possibility of a different reaction pathway. MO calculations have been carried out to obtain more insight into the observed reactivity of [Ni(dsdm)] and [Ni(dsdm-O_2)].

Theoretical Details. Chemical computations were used to address issues relating to the difference between the levels of S-oxygenation in the various N_2S_2Ni complexes [Ni(dsdm)], [Ni(dspm)], and [Ni(bme-daco)]. Molecular mechanics calculations using the open force field (OFF) program with the universal force field (UFF) and QEq calculated atomic charges as implemented in Cerius^{2} [46] were used to probe whether the ligands dspm and bme-daco might prohibit the rearrangement required in the formation of the octahedral disulfonato complex. Comparisons of the space-filling models derived for the hypothetical six-coordinate disulfonate structures based on daco and dspm with the actual octahedral structure of complex **5** found little difference among the three structures. All of the changes as the square-planar *cis*-N_2S_2 ligands are converted into *trans*-$(O_2SO)_2NiN_2(H_2O)_2$ reside in the S to N chain; there are no obvious prohibitive steric interactions or structural strains in the more rigid ligand. Thus, it appears that both the daco mesocyclic ligand system and the dspm ligand should be able to accommodate the fully oxygenated $N_2S_2O_6Ni$ product.

Since the molecular mechanics calculations do not indicate any prohibitive steric interactions in the hypothetical product with daco and dspm, DFT calculations using the modified LANL2DZ basis set at the B3LYP level of theory were used to investigate the electronic character of the three monosulfinate complexes **4**, [Ni(dspm-O_2)], and [Ni(mese-daco)]. B3LYP-optimized structures were determined for these sulfinato complexes, and for comparison also for the non-oxidized complexes [Ni(dsdm)], [Ni(dspm)], and [Ni(bme-daco)]. Coordinates for [Ni(dsdm-O_2)], [Ni(dspm)],[35] [Ni(bme-daco)], and [Ni(mese-daco)][15] were derived from X-ray structures. Starting coordinates for [Ni(dsdm)] were taken from the monosulfinate complex [Ni(dsdm-O_2)], while for [Ni(dspm-O_2)] these were derived from the X-ray structure of the nonoxidized compound [Ni(dspm)] (CCDC_KIGYEE)[35] as no data set is available yet for [Ni(dspm-O_2)].

The metric data derived from the X-ray crystal structure and from the B3LYP-optimized geometry of the monosulfinate complex [Ni(dsdm-O_2)] with the staggered N to S linkers (N−C−C−S) in our study are in good agreement throughout the distances and angles chosen for analysis. The staggered structure for [Ni(dsdm-O_2)] was found to be 4.6 kcal/mol lower in energy than the eclipsed conformation, consistent with the experimental observation of only the staggered conformer from the solid-state structure. In the case of [Ni(dsdm)], for which no crystal structure is available yet, the staggered conformation is shown to be 3.6 kcal/mol lower than the eclipsed complex. The B3LYP-calculated geometries for [Ni(bme-daco)] and [Ni(mese-daco)] are not in as good agreement with the X-ray data due to experimental (crystallographic) uncertainties in the orientation of the N to S linkers. The B3LYP-calculated energy for the staggered conformation is lower in energy than the eclipsed conformation by less than 1 kcal/mol for both [Ni(bme-daco)] and [Ni(mese-daco)] compounds, which is within the uncertainty of this level of theory. Good agreement was also found for data of both [Ni(dspm)] and [Ni(dspm-O_2)], which were compared with the [Ni(dspm)] X-ray crystal data. The eclipsed structures for [Ni(dspm)] and [Ni(dspm-O_2)] were calculated to be 4.1 and 1.4 kcal/mol lower in energy, respectively, than the staggered conformation. These results indicate that the B3LYP level of theory with the basis set used gives a good representation of these types of compounds.

The 0.05 contour surface diagrams for the highest occupied molecular orbital (HOMO) and lowest unoccupied molecular orbital (LUMO) of all three sulfinato species [Ni(dsdm-O_2)], [Ni(dspm-O_2)], and [Ni(mese-daco)] are shown in Figure 3, and are highly similar for all three complexes. For each of these complexes the LUMO is characterized by a Ni($d_{x^2-y^2}$) antibonding interaction with the p-orbitals of the sulfur and

(45) Grapperhaus, C. A.; Maguire, M. J.; Tuntulani, T.; Darensbourg, M. Y. *Inorg. Chem.* **1997**, *36*, 1860.
(46) Accelrys, Inc. *Cerius2 Force-Field Based Simulations*, Release 4.2; Accelrys Inc.: San Diego, 2000.

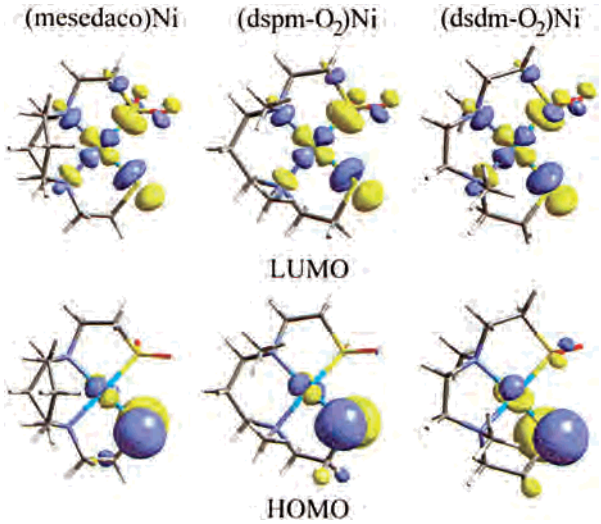

Figure 3. HOMO and LUMO diagrams of the monosulfinate complexes.

nitrogen donors in the N_2S_2 molecular plane. The HOMOs for [Ni(dspm-O_2)] and [Ni(mese-daco)] molecules are characterized by the antibonding thiolate S(p_z)/Ni(d_{xz}) interactions, with minimal contributions from the orbitals of oxygen and carbon atoms α to the thiolate sulfur. The HOMO for [Ni(dsdm-O_2)] differs in that there is mixing of Ni(d_{z^2}) with Ni(d_{xz}), which forms the antibonding interaction with thiolate S(p_z). This results in one, mainly d-orbital, lobe pointing away from the large p_z-orbital on the thiolate ligand, making the HOMO more accessible for substrate interaction. The [Ni(dspm-O_2)] sulfinato complex has previously been subjected to a theoretical analysis by Maroney et al.[39] In these earlier computations, the major contributor to the HOMO consisted primarily of the p-orbital on the sulfinato oxygen, and the LUMO was essentially of Ni(p_z) character.[39] The lack of reactivity of molecular oxygen with the remaining thiolate of [Ni(dspm-O_2)] was attributed to this sulfinato-based HOMO. However, in these calculations a standard double-ζ basis set (LANL2DZ) was used on all atoms, neglecting the d-orbitals on sulfur, and the calculations were performed at the Hartree−Fock level of theory, which neglects correlation effects. The sulfur basis set used in these calculations includes a d-function (polarization function) on sulfur, required for expansion of the valency in the sulfur donor RSO_2 ligand. The differences in the d-orbital makeup of the HOMOs led us to explore consequences of the reaction of [Ni(dsdm-O_2)] with ground-state molecular oxygen in terms of possible adducts as follows.

Figure 4 displays three possible O_2 adducts of [Ni(dsdm-O_2)] as fully optimized, B3LYP, structures. Structures **A** and **B** differ from each other in the approach of O_2 on alternate sides of the N_2S_2 plane. The more exothermic arrangement **A** results from access to the more open side of the Ni_d/thiolate S(p_z) antibonding interaction. In each case, the dioxygen molecule lies along the Ni−SO_2 bond vector. Every attempt was made to find local minima with the O_2 parallel or proximate to the Ni−S (thiolate) bond; optimization returned to **A** or **B**. Structure **C** is that of the O_2 interaction at the thiolate sulfur, which makes very weak interactions with an H-atom on the α-carbon. The small energy differences in

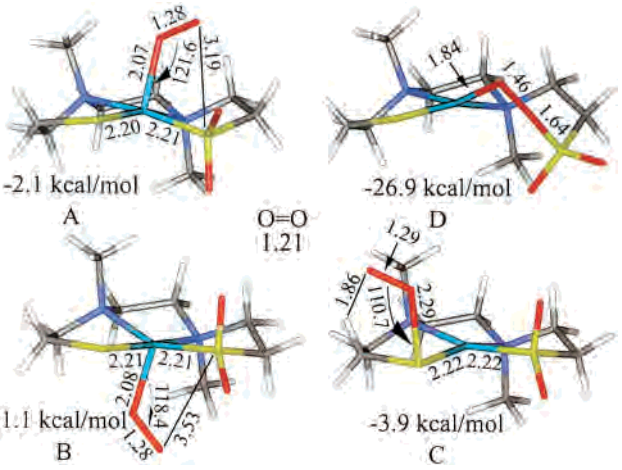

Figure 4. Possible O_2 adducts of [Ni(dsdm-O_2)].

Scheme 3

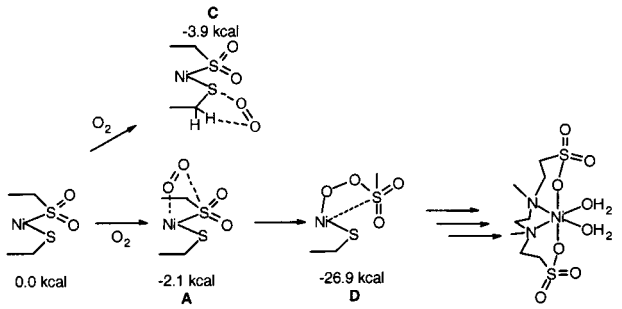

A−**C** are within the error of this level of theory. From these calculated structures two possible routes to the fully oxygenated disulfonate complex can be postulated. It can be envisaged that following structure **C** a nickel disulfinate complex would be formed. However, the fact that this assumedly relatively stable intermediate nickel disulfinate complex could not be isolated may suggest that it is not on the route to the fully oxidized disulfonate complex. Following structure **A**, insertion of O_2 would lead to a Ni−O−O−SO_2R species as calculated in structure **D**. The oxygen now acts as a nucleophile accessing the LUMO of the nickel complex. As shown in Scheme 3, the large exothermicity indicates a favorable step. The advantage of this intermediate is that only one nickel−sulfur bond has to be broken in the same step. This calculated intermediate species is expected to be a potent oxidant, and subsequent steps would involve O-atom transfer from the highly reactive peroxy species in intra- or intermolecular processes to available oxophiles, i.e., the unoxidized sulfur atom.

Comments

It has been assumed that the formation of a monosulfinato complex from nickel *cis*-dithiolate complexes is a result of nucleophilic attack by the thiolate sulfur on the electrophilic O_2 molecule. The difference in bonding character from RS^- vs $RS(=O)_2^-$ leads to such a dramatic lowering of the nucleophilicity of the remaining, nonoxidized thiolate that it is unreactive toward molecular oxygen, should the same reaction path as in the first oxygenation (nucleophilic attack of RS^- on O_2) be operative.[39,45] In fact, reaction of the [Ni-

Scheme 4

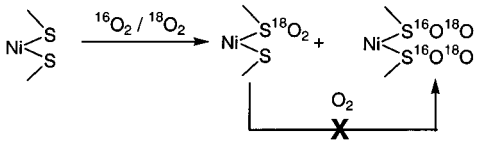

(bme-daco)] complexes with isotope-labeled $^{18}O_2$ showed that the monosulfinate complex was formed by molecular O_2 addition at a single thiolate sulfur, whereas the disulfinato complex is formed by a cross-site, molecular O_2 addition, with a disulfenato species as an intermediate (Scheme 4).[15] Both products are derived from the initial Ni-bound RS−O−O$^-$ persulfoxide species, and the divergent mechanistic pathway accounts for the two products.

As presented in this paper, the thiolato sulfurs of [Ni(dsdm)] react with molecular oxygen to yield the fully oxidized [Ni(dsdm-O_6)(H_2O)$_2$]. Such reactivity is apparently not possible for the related complexes [Ni(dspm)] and [Ni(bme-daco)]. Despite this, the molecular mechanics calculations suggest that the fully oxygenated forms of the ligands dspm and bme-daco should be able to accommodate an octahedral geometry of the nickel ion similar to that observed for [Ni(dsdm-O_6)(H_2O)$_2$]. A comparison of the crystal structure for the dimethylated complex [Ni(Me_2-dsdm)I_2] with that of the bme-daco-derived complex[36] shows that, upon reaction with methyl iodide, [Ni(dsdm)] converts to the octahedral complex [Ni(Me_2-dsdm)I_2], with the thioether S-donors coordinating in the axial positions. In contrast, the thioether donors in [Ni(Me_2bme-daco)]I_2 remain coordinated as they were in the *cis*-dithiolate complex, thereby keeping the nickel ion in a low-spin square-planar geometry.[36] These results indicate that the barrier to form an octahedral complex is too high for the bme-daco backbone. A similar reason could be envisaged for the hypothetical disulfonato complexes derived from [Ni(dspm)] and [Ni(bme-daco)]. Although the molecular mechanics calculations indicate that a hypothetical six-coordinate disulfonate structure is possible for [Ni(dspm)] and also for [Ni(bme-daco)], there seems to be an energy barrier for the reaction to these complexes that cannot be overcome, as no disulfonato complexes are formed in both cases. Considering the available data, no obvious reasons can be postulated which explain the difference in reactivity among [Ni(dsdm)], [Ni(dspm)], and [Ni(bme-daco)]. The only difference observed, as shown by the DFT calculations, is a slightly more accessible HOMO for substrate interaction for [Ni(dsdm-O_2)], compared to [Ni(dspm-O_2)] and [Ni(mese-daco)].

Finally, the competence of [Ni(dsdm-O_2)] as an intermediate for further reaction with O_2 has been demonstrated, which invokes a new mechanistic route for extensive oxygenation of metal-bound sulfur ligands, as nucleophilic attack on dioxygen by the deactivated thiolato sulfur is not viable. This deactivation is demonstrated by the above-described calculations and the fact that no further reactivity is observed for [Ni(dspm-O_2)] and [Ni(mese-daco)]. The DFT calculations as presented here show a possible intermediate toward the fully oxygenated product starting from [Ni(dsdm-O_2)]. The results are consistent with a switch in reactivity of O_2 with the complex [Ni(dsdm-O_2)], following the first (electrophilic) addition of O_2 to the (nucleophilic) thiolate sulfur of [Ni(dsdm)]. We suggest that the resultant electrophilicity of the Ni−SO_2R bond site elicits the nucleophilic reactivity character of O_2, and provides a path for a four-centered peroxy intermediate or transition state. This results in subsequent and irrevocable oxygenation steps. Such cooperativity or cascading dioxygen addition reactivity leads to the fully oxidized product [Ni(dsdm-O_6)(H_2O)$_2$]. The use of a sterical hindered version of [Ni(dsdm)] could provide additional information about the obtained reactivity.

Acknowledgment. Financial support for this project has been provided by the Netherlands Foundation for scientific research (NWO), through SIR Grant No. 13-4310, and by the National Science Foundation, Grants CHE-9812355 and CHE 85-13273 for the X-ray diffractometer and crystallographic computing system. We thank the supercomputing facility at Texas A&M University for computer time and the Laboratory for Molecular Simulation at Texas A&M University for software and computer time.

Supporting Information Available: X-ray crystallographic files, in CIF format, and Figure S1 giving a representation of the hydrogen bonds present in compound **4**. This material is available free of charge via the Internet at http://pubs.acs.org.

IC010784X